Journal of Sound and Vibration 443 (2019) 238–252

Contents lists available at ScienceDirect

Journal of Sound and Vibration

journal homepage: www.elsevier.com/locate/jsvi

Convective correction of metafluid devices based on Taylor transformation

Umberto Iemma *, Giorgio Palma

University of Roma Tre, Department of Engineering, 00146, Rome, Italy

ARTICLE INFO

Article history:
Received 19 June 2018
Revised 9 November 2018
Accepted 27 November 2018
Available online 29 November 2018
Handling Editor: Y. Auregan

Keywords:
Metamaterials
Metafluids
Taylor transformation
Aeroacoustic cloaking
Transformation acoustics
Convective acoustic metamaterial

ABSTRACT

The paper presents a method to modify the mechanical properties of a statically–designed metamaterial device in order to preserve its performance when operating in a non–uniform aerodynamic flow. The objective of the research is to contribute to the disclosure of the acoustic metamaterial potential in aeroacoustic applications, where acoustic propagation and scattering are deeply affected by aerodynamic convection. The emphasis is on aeronautical applications aiming at the development of methods for the design of breakthrough solutions for aircraft noise mitigation. The present approach is based on the application of the inverse Taylor transformation to the static design space in order to obtain the properties of an equivalent metamaterial in the convected space. The metamaterial so–obtained is capable to guarantee the target acoustic response in presence of a non–uniform background flow at low Mach number and with negligible vorticity. Numerical results obtained through finite–element simulations are presented for a free stream Mach number ≤ 0.35, which is compatible with the take–off and landing operation of a commercial airplane. The benchmark used is the widely assessed problem of the scattering cancellation (cloaking) of a circular obstacle. The acoustic disturbance is here assumed to be generated by an isotropic point source located in the vicinity of the scatterer and co–moving with it. The numerical results reveal that the effect of the proposed correction strongly depends on the relative position of the source and the metamaterial device, with the worst performance obtained when they are aligned with the free stream. The reason of this dependence is analytically explained and verified numerically. When the alignment of the source and the treated object is orthogonal to the flow, the Taylor–corrected metamaterial recovers almost completely its expected behaviour. This result makes the approach appealing for all those engineering applications where the relative position of sources and moving boundaries is fixed and compatible with the most favourable conditions.

1. Introduction

Acoustic metamaterials is nowadays probably the most lively topic in acoustic research. A simple search of the scientific databases with the keywords *metamaterial*, *metasurfaces* and *acoustics* produces more than one thousand results, with an increase of the number of contributions per year of one order of magnitude since 2007. Repeating the same search adding the prefix *aero* to the last keyword produces a drop down of the entries to less than ten. The reasons behind this substantial

* Corresponding author.
E-mail addresses: umberto.iemma@uniroma3.it (U. Iemma), giorgio.palma@uniroma3.it (G. Palma).

https://doi.org/10.1016/j.jsv.2018.11.047

difference can be many, starting from the fact that the research community in aeroacoustics is certainly less numerous than that in general acoustics. One motivation among others can be related to the fact that most of the metamaterial modeling techniques developed during the first decade of the 21st century where inherited from the electromagnetism context, relying on the formal analogy, under specific assumptions, of the Maxwell equations with the mass and momentum conservation laws of a compressible medium undergoing small, zero-mean perturbations of its status (Cummer and Shurig [1]). Indeed, the term metamaterial, first used by Walser [2] for man-made materials engineered with a specific response not available in nature, was adopted in optics and electromagnetism to identify materials capable to realise the total control of electromagnetic scattering, made possible by the coordinate transformation approach (Pendry, Schurig & Smith [3] and Leonhardt [4]). After the Cummer and Shurig paper [1], where the applicability of the same concept in acoustics was first demonstrated, the number of contributions aiming at the actual realization of metamaterials has grown considerably, witnessing the tremendous interest of the research community on the virtually uncountable possibilities introduced by the so–called Standard Transformation Acoustic (STA). Among the substantial literature produced in the last ten years, it is worth mentioning here the extensive contribution by Sanchez–Dehesa and his collaborators that led to the practical realization of concepts such as acoustic cloaking devices [5,6] and acoustic lenses [7]. Of particular relevance for the present paper is the milestone work by Norris [8,9] who developed the formalisms of the STA, with a special emphasis on the acoustic cloaking, and presented, for the first time, the most general equation governing the propagation of acoustic waves in metamaterials, introducing the concept of metafluid.

One of the main limitations of the classic approach to metamaterial design is the underlying assumption that the fluid in which the acoustic perturbation propagates and the obstacles in it must be at rest. While this hypothesis is not a great limitation in the acoustic domain, it is clearly not acceptable in aeroacoustics and aeronautical applications. Dealing in particular with the STA, its extension to the aeroacoustic domain is not trivial. The difficulties that arise are intrinsic in the structure of the governing equations in the presence of flow: the convective terms that appears mix time and space derivatives, making the equations no longer formally invariant under coordinate transformations and the approach consequently fails.

Some attempts to overcome such limitation can be found in literature. The most relevant, to the authors' opinion, is the work by Huang et al. [10], where a simple Doppler–like correction is applied to the static design to obtain an improvement of the cloaking capability of the device when the object is in relative motion with respect to the surrounding medium and impinged by a planar acoustic perturbation. However, the Mach number in the presented simulations is limited to 0.06, too far from realistic aeroacoustic scenarios. A closely related correction for the static metamaterial design is resumed in Iemma [11], where a local Doppler–like correction is introduced, based on the local wave vector of the incoming acoustic perturbation induced by a source in the proximity of the scatterer and co–moving with it. This correction is applicable to situations where the distance between source and obstacle is such that the assumption of planar wave fronts is not acceptable. Numerical results confirming the validity of the approach are presented for Mach numbers up to 0.2, even if the simplifying assumption of uniform background flow is considered, neglecting the aerodynamic perturbation induced by the scatterer. A numerical optimization approach to the aeroacoustic cloaking is presented in Zhong & Huang [12]. The procedure is capable to attain an optimized metamaterial design in the presence of an arbitrarily complex turbulent flow. The optimality of the solution holds only for the specific flow conditions analysed and hence requires, for practical application, the availability of real time flow estimate and tunable metamaterial devices. Despite this practical limitation, this contribution is, to the authors' knowledge, the only available attempt to address the problem of metamaterial operating in complex flows.

A completely new design framework was presented by García–Meca and his collaborators [13–16] as an alternative to the STA capable to deal with moving medium. The Analogue Transformation Acoustics (ATA) extends the classic transformation method to handle arbitrary space–time coordinate transformations and design metamaterial devices in presence of background aerodynamic flows. The convective form of the wave equation is rewritten in the four–dimensional space–time and its relativistic structure is exposed and exploited. However, till now, just few aeroacoustic applications, *e.g.,* cloaking of a small bump on a flat wall using a quasi–conformal coordinate transformation, were tested by the authors. Furthermore, Iemma & Palma [17,18] showed how the application of the method in combination with quasi–conformal transformations is not able to achieve perfect omnidirectional cloaking for objects fully immersed in the hosting fluid and that the method produces a non–physical velocity field inside the cloak domain, compared with a simple potential solution around the cloaked object.

Recently, Ryoo & Jeon [19] developed an acoustic analogy for the hosting medium that considers and shows the contribution to the scattering pattern of non uniformity and compressibility of the background flow, in combination with an optimization approach, similar to the work by Huang [12]. Their research goal is to obtain a deeper knowledge of the effects of compressibility and non–uniformity of the flow in the scattering phenomenon and to improve the effectiveness of the optimized devices including more terms in the adopted acoustic analogy.

In the present paper, a general method for the convective correction of static metamaterial design is presented. The method aims at the identification of the mechanical properties that the metamaterial device should exhibit in order to preserve its efficiency when operating in a flow. The approach is based on the application of the inverse Taylor transformation in the domain occupied by the metamaterial. The metamaterial is modelled as a metafluid, following the theoretical model proposed by Norris [9]. The metafluid device is assumed to be impermeable, and the material at rest. The use of the inverse transformation guarantees that the propagation of pseudo–acoustic field inside the quiescent metamaterial is distorted to match the pressure distribution induced at its outer boundary by a moving medium. In order to mimic the typical situation arising in aeronautical applications, the external primary acoustic field is assumed to be generated by a point source co–moving with the metamate-

rial device, located at a distance such that the wave fronts cannot be considered planar. The design correction is applicable, in principle, to any metamaterial–based device, independently of its specific functionality and the methodology used for the static design. The present approach follows the acoustic analogy presented in Iemma & Burghignoli [20] and Iemma [11]. All the terms taking into account the acoustic behaviour of the metafluid are interpreted as equivalent sources for the standard wave equation consisting in a monopole and a dipole contribution.

The benchmark problem used here is the inertial–cloaking of a sound–hard cylindrical obstacle impinged by a uniform stream. Despite the low–Mach number assumption on the basis of the Taylor transformation, the validity of the correction is verified for Mach number values up to 0.35, to comply with the take-off and landing conditions of commercial aircraft and for reduced frequency ≤4. The paper is organized as follows: Section 2 recalls the structure of the Taylor transformation which is applied to the equations governing the acoustics of metafluids in Section 3. The nomenclature used complies as much as possible to the ones used in the original works of Taylor [21] and Norris [9] to help the reader in the interpretation of the method. Section 4 is dedicated to the presentation and comment of the numerical simulations including some considerations about the possibility to realise in practice the design obtained with the present method. The conclusions are drawn in Section 5.

2. The Taylor transformation

In 1978, Taylor introduced a coordinate transformation to analyse the effect of a non–uniform flow on the propagation of an acoustic perturbation [21] aiming at the development of tools for the interpretation of low–speed, wind–tunnel aeroacoustic experiments or the correction of static measurements. Let's consider a uniform stream of a compressible medium impinging an impermeable obstacle, and undergoing unsteady, zero–mean, small perturbations of pressure and density induced by an acoustic source. In this condition, the velocity of a particle can be expressed as the superposition of three components: the uniform speed of the stream at infinite distance from the obstacle, $\mathbf{v}_\infty$, the perturbation velocity $\mathbf{u}$ induced by the presence of the impermeable object, and the zero–mean velocity induced by the acoustic perturbation. Taylor transformation is based on the approximation of the convective wave equation to order $\mathcal{O}(M_\infty)$, being $M_\infty = \left\|\mathbf{v}_\infty\right\| / c_\infty$ the asymptotic Mach number under the assumption for the aerodynamic velocity field to be potential

$$\left(\frac{\partial^2}{\partial t^2} + 2M_\infty \nabla\widehat{\Phi}\cdot\nabla\frac{\partial}{\partial t} - c_\infty^2\nabla^2\right)\varphi = S(\mathbf{x},t), \tag{1}$$

where c_∞ is the speed of sound at infinity, Φ is the aerodynamic velocity potential, such that $\mathbf{v}_0 = \mathbf{v}_\infty + \mathbf{u} = \nabla\Phi$ (with $\widehat{\Phi} = \Phi/\left\|\mathbf{v}_\infty\right\|$), and φ is the acoustic velocity potential generated by the source distribution S. The condition for φ on the boundary $\Gamma(\mathbf{x})$ of an acoustically rigid object is

$$\nabla\varphi\cdot\nabla\Gamma = 0 \quad \text{on} \quad \Gamma(\mathbf{x}) = 0, \tag{2}$$

$$\text{and} \quad \varphi = \frac{\partial\varphi}{\partial t} = S = 0 \quad \text{when} \quad t < t_0 - \frac{M_\infty\widehat{\Phi}}{c_\infty}. \tag{3}$$

In the case of aerodynamic impermeability of the boundary Γ, the condition on $\widehat{\Phi}$, which satisfies the $\nabla^2\widehat{\Phi} = 0$, is

$$\nabla\widehat{\Phi}\cdot\nabla\Gamma = 0 \quad \text{on} \quad \Gamma(\mathbf{x}) = 0, \tag{4}$$

$$\text{and} \quad \widehat{\Phi} \approx \mathbf{x} \quad \text{as} \quad r\to\infty \tag{5}$$

where $r \equiv |\mathbf{x}| \equiv \sqrt{x^2+y^2+z^2}$. Taylor transformation consists in applying a time shift not uniform in space, depending on the aerodynamic potential of the background flow. The coordinate transformation has the form

$$\left(\overline{\mathbf{x}},\overline{t}\right) = \left(\mathbf{x}, t + \frac{M_\infty\widehat{\Phi}}{c_\infty}\right), \quad \varphi(\overline{\mathbf{x}},\overline{t}) = \varphi(\mathbf{x},t), \tag{6}$$

where $\overline{\mathbf{x}},\overline{t}$ represent an event in the transformed space–time. The relationships between the differential operators in the two spaces are

$$\frac{\partial}{\partial t} = \frac{\partial}{\partial\overline{t}}, \qquad \nabla = \overline{\nabla} + \nabla\widehat{\Phi}\frac{M_\infty}{c_\infty}\frac{\partial}{\partial\overline{t}},$$

$$\nabla^2 = \overline{\nabla}^2 + 2M_\infty\nabla\widehat{\Phi}\cdot\overline{\nabla}\frac{\partial}{c_\infty\partial\overline{t}} + \frac{M_\infty^2|\nabla\widehat{\Phi}|^2}{c_\infty^2}\frac{\partial^2}{\partial\overline{t}^2} \tag{7}$$

where $\overline{\nabla}$ indicates differentiation with respect to $\overline{\mathbf{x}}$. Clearly, Eqs. (1) and (6) yield, within the order M_∞ approximation, to

$$\left(\frac{\partial^2}{\partial\overline{t}^2} - c_\infty^2\overline{\nabla}^2\right)\varphi = S(\overline{\mathbf{x}},\overline{t}) \tag{8}$$

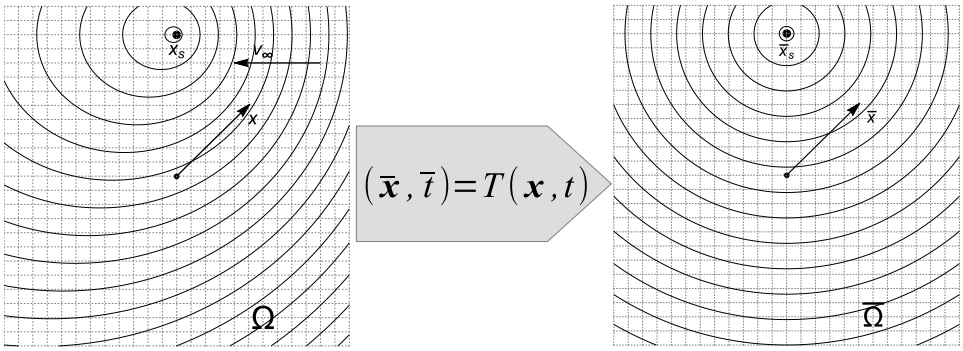

Fig. 1. Effect of the Taylor transformation on the field induced by a point source in $\mathbf{x}_s \in \Omega$ surrounded by a uniform stream at speed $\mathbf{v}_\infty$. In the virtual space $\overline{\Omega}$ the wave fronts (black curves) recover the isotropic propagation pattern of the stationary case.

i.e., the convected wave equation in the physical space is transformed into the classic wave equation for a medium at rest in a virtual space (see Fig. 1).

Taylor has shown how the transformation presented can be used, in the spectral domain, to find the relationship between the complex amplitude of the static acoustic potential $\widetilde{\varphi}_s$ and that of the convected field. The resulting correction reads

$$\widetilde{\varphi}(\mathbf{x}, \omega) = \widetilde{\varphi}_s(\overline{\mathbf{x}}, \omega) e^{-ik_\infty M_\infty \hat{\Phi}(\overline{\mathbf{x}})} \tag{9}$$

where ω is the angular frequency and $k_\infty = \omega / c_\infty$.

3. Aeroacoustic correction of metafluids' properties

Adopting the formalism introduced by Norris [8], the propagation of an acoustic perturbation p in a quiescent metafluid can be described by

$$\mathcal{K}\,\mathbf{Q}{:}\nabla\left(\boldsymbol{\rho}^{-1}\,\mathbf{Q}\,\nabla p\right) - \frac{\partial^2 p}{\partial t^2} = 0. \tag{10}$$

The above equation encompasses all the characteristics of a metamaterial capable of an arbitrary pseudo–acoustic behaviour. Both density and stiffness are assumed to be anisotropic, represented by the tensors $\boldsymbol{\rho}$ and $\mathcal{K}\mathbf{Q}$, respectively, where $\mathbf{Q}$ can be any symmetric tensor such that $\nabla \cdot \mathbf{Q} = 0$. The Cauchy stress tensor for such a material is given by $\boldsymbol{\sigma} = -p\mathbf{Q}$, where the pseudo–pressure p is related to the strain tensor $\boldsymbol{\epsilon}$ by $p = -\mathcal{K}\,\mathbf{Q}{:}\boldsymbol{\epsilon}$. The STA approach starts from the assumption that a physical domain Ω_c occupied by the metamaterial device can be obtained applying a coordinate transformation $\mathbf{x} = f(\breve{\mathbf{x}})$ to the virtual domain $\breve{\Omega}$ where no obstacle is present and the wave fronts can propagate freely. Transformation $\mathbf{x} = f(\breve{\mathbf{x}})$ is such that the boundary of the obstacle in Ω_c is mapped onto a point in $\breve{\Omega}$, thus achieving the appropriate distortion of the wave pattern. The mechanical properties of the metamaterial, $\mathcal{K}$ and $\boldsymbol{\rho}$, can be obtained as

$$\mathcal{K} = \mathcal{K}_{\text{ref}} J, \quad \boldsymbol{\rho} = \rho_{\text{ref}} J \mathbf{Q} (\mathbf{D}\mathbf{D}^T)^{-1} \mathbf{Q}^T \tag{11}$$

where $\mathcal{K}_{\text{ref}}$ and ρ_{ref} are the bulk modulus and the density of the reference medium, $\mathbf{D} = \breve{\nabla} f(\breve{\mathbf{x}})$, $J = \det(\mathbf{D})$, and $\breve{\nabla}$ indicates the differentiation with respect to $\breve{\mathbf{x}} \in \breve{\Omega}$, *i.e.,* in the virtual domain. The metamaterial design so obtained can achieve the desired meta–behaviour only when the host medium is at rest, and the presence of a background flow has been demonstrated to deteriorate significantly the performance of the device. Indeed, when Eq. (10) is coupled with the convective equation of the acoustic propagation in the hosting fluid, the boundary conditions cannot be fulfilled anymore making the static design ineffective. The acoustic propagation in Ω_h in presence of the vorticity–free flow of a barotropic, inviscid fluid is governed by

$$-\frac{\partial}{\partial t}\left[\frac{\rho_0}{c_0^2}\left(\frac{\partial \varphi}{\partial t} + \mathbf{v}_0 \cdot \nabla \varphi\right)\right] + \nabla \cdot \left[\rho_0 \nabla \varphi - \frac{\rho_0}{c_0^2}\left(\frac{\partial \varphi}{\partial t} + \mathbf{v}_0 \cdot \nabla \varphi\right)\mathbf{v}_0\right] = 0 \tag{12}$$

where φ is the acoustic potential, $\mathbf{v}_0$, ϱ_0 and c_0 are the mean–flow velocity, local density and speed of sound, respectively. The method presented here aims at the recovery of the capacity of the metamaterial capacity to attain the desired acoustic response in presence of flow by introducing a correction of its mechanical properties based on the inverse Taylor transformation. The metamaterial that constitutes the device is assumed to be at rest and its outer boundary to be impermeable. The transformation is applied in the domain Ω_c occupied by the metafluid (see Fig. 3 for domain nomenclature), where no aerodynamic flow is permitted. The Bernoulli's equations in frequency domain reads $\widetilde{p} = i\omega\varrho_{\text{ref}}\widetilde{\varphi}$, and thus Eq. (9) holds in Ω_c for pressure as well, to yield an inverse relationship for the pressure that reads

$$\widetilde{p}_s(\mathbf{x}, \omega) = \widetilde{p}(\mathbf{x}, \omega) e^{A(\mathbf{x})} \tag{13}$$

where the imaginary function $A(\mathbf{x}) = i\,k_\infty M_\infty \Phi(\mathbf{x}) / v_\infty$ is introduced for the sake of notational simplicity.

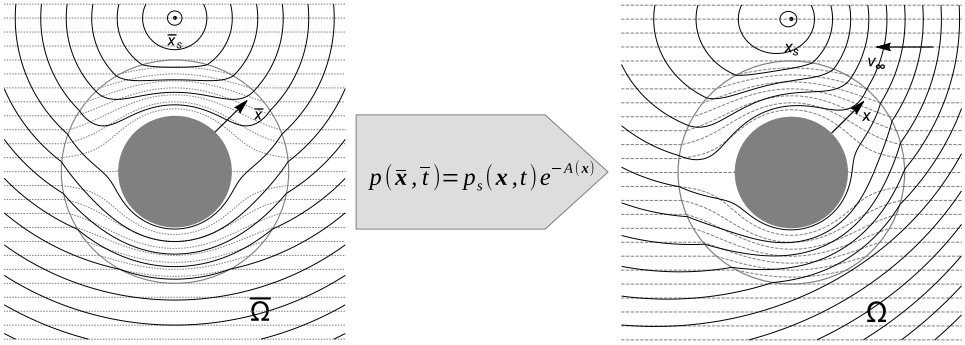

Fig. 2. Sketch of the effect of the inverse Taylor mapping: resulting wavefronts mimic the presence of a background flow.

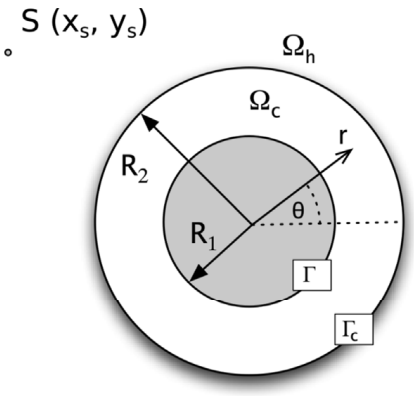

Fig. 3. Nomenclature used for the computational domain.

Fig. 2 sketches how inverse Taylor transform changes the shape of the static solution in Ω_c so as to make it compatible (to the order of M_∞) with the convective acoustic field in Ω_h. As a consequence, the continuity condition at the boundary between the cloak and the field can now be fulfilled and the scattering cancellation preserved. Now, the question the present work is trying to answer is: what should the mechanical parameters of the metamaterial be to guarantee a convective–like propagation pattern without a background flow? In order to answer this question, Eq. (13) is combined with the Fourier transform of Eq. (10). Let's consider the tensor differential identity (see, *e.g.,* Gurtin [22]) $\nabla\cdot\left(\mathbf{S}^T\mathbf{w}\right)=\mathbf{S}:\nabla\mathbf{w}+\mathbf{w}\cdot(\nabla\cdot\mathbf{S})$ where $\mathbf{S}$ is a generic second–order tensor and $\mathbf{w}$ is a vector, and apply this identity to the first term of Eq. (10) with $\mathbf{S}=\mathbf{Q}$ and $\mathbf{w}=\varrho^{-1}\mathbf{Q}\nabla p$. Taking into account that $\mathbf{Q}\in Sym$ and is divergence–free by definition, it follows[1]

$$\mathbf{Q}:\nabla\left(\varrho^{-1}\,\mathbf{Q}\,\nabla p\right)=\nabla\cdot\left(\mathbf{Q}\varrho^{-1}\,\mathbf{Q}\,\nabla p\right) \tag{14}$$

Substituting this result in Eq. (10), indicating with $\widetilde{p}_s$ the Fourier transform of the acoustic disturbance propagating in static conditions yields

$$\mathcal{K}_s\,\nabla\cdot\left[\mathbf{Q}\varrho_s^{-1}\,\mathbf{Q}\,\nabla\left(\widetilde{p}_s e^{-A(\mathbf{x})}\right)\right]+\omega^2\left(\widetilde{p}_s e^{-A(\mathbf{x})}\right)=0 \tag{15}$$

Starting from this equation, the idea is to guarantee *convective–like* propagation patterns inside Ω_c with a static meta–medium having mechanical properties suitably modified so as to make Eq. (15) satisfied. The spatial dependence of the correction factor implies

$$\nabla\cdot\left[e^{-A(\mathbf{x})}\mathbf{Q}\varrho_s^{-1}\,\mathbf{Q}\left(\nabla\widetilde{p}_s-p_s\nabla A\right)\right]+\frac{\omega^2}{\mathcal{K}_s}\widetilde{p}_s e^{-A(\mathbf{x})}=\nabla\cdot\left[\mathbf{Q}\varrho_T^{-1}\,\mathbf{Q}\left(\nabla\widetilde{p}_s-p_s\nabla A\right)\right]+\frac{\omega^2}{\mathcal{K}_T}\widetilde{p}_s=0 \tag{16}$$

where the corrected inertia tensor $\varrho_T=\varrho_s\,e^{A(\mathbf{x})}$ and bulk modulus $\mathcal{K}_T=\mathcal{K}_s\,e^{A(\mathbf{x})}$ are introduced. It is interesting to notice that the application of the inverse Taylor transformation to Eq. (10) yields mechanical properties corrected by the direct transformation. Using the acoustic analogy approach (see, Iemma and Burghignoli [20] and Iemma [11]), Eq. (16) can be rearranged to recast the static wave operator on the left hand side, and move to the right hand side the terms that model the behaviour of the metafluid in Ω_c. This results in a field distribution of monopoles and dipoles that is expected to yield the target meta-behaviour. Summing

[1] It should be noted that the conditions $\mathbf{Q}\in Sym$ and $\nabla\cdot\mathbf{Q}=0$ make the use of the tensor contraction in Eq. (10) not necessary.

and subtracting the terms $\omega^2\widetilde{p}/\mathcal{K}_{\text{ref}}$ and $\nabla^2\widetilde{p}$ in Eq. (16) and observing that $\nabla^2\widetilde{p} = \nabla\cdot(\mathbf{I}\nabla\widetilde{p}) = \mathbf{I}{:}\nabla\left(\nabla\widetilde{p}\right)$, one obtains

$$\nabla^2\widetilde{p} + \frac{\varrho_{\text{ref}}}{\mathcal{K}_{\text{ref}}}\,\omega^2\widetilde{p} = \nabla\cdot\widetilde{\mathbf{q}}\,(\mathbf{x},\omega) + \widetilde{\sigma}\,(\mathbf{x},\omega) \tag{17}$$

where

$$\begin{aligned}\widetilde{\mathbf{q}}\,(\mathbf{x},\omega) &= \left(\mathbf{I} - \mathbf{Q}\widehat{\boldsymbol{\varrho}}_{_T}{}^{-1}\mathbf{Q}\right)\,\nabla\widetilde{p} + \mathbf{Q}\widehat{\boldsymbol{\varrho}}_{_T}{}^{-1}\mathbf{Q}\,\nabla A\,\widetilde{p}\\ \widetilde{\sigma}\,(\mathbf{x},\omega) &= \varrho_{\text{ref}}\,\omega^2\left(\frac{1}{\mathcal{K}_{\text{ref}}} - \frac{1}{\mathcal{K}_{_T}}\right)\widetilde{p}\end{aligned} \tag{18}$$

with $\widehat{\boldsymbol{\varrho}}_{_T} = \boldsymbol{\varrho}_{_T}/\varrho_{\text{ref}}$. It is worth noting that no assumptions are made here about the method used to define the tensors characterizing the metafluid. Indeed, the approach presented in this paper can be used to correct any static metafluid design, independently of the specific methodology used for its derivation, the only limitation being the assumption of a potential aerodynamic flow. This assumption will be discussed later, when some considerations about the actual realisability of the correction are made.

4. Numerical simulation

In the present work, for the sake of simplicity and without loss of generality, we will limit our numerical analysis to the case $\mathbf{Q} = \mathbf{I}$, *i.e.,* the so–called inertial cloaking. In this case, the equivalent sources in Eq. (18) reduce to

$$\begin{aligned}\widetilde{\mathbf{q}}\,(\mathbf{x},\omega) &= \left(\mathbf{I} - \widehat{\boldsymbol{\varrho}}_{_T}{}^{-1}\right)\,\nabla\widetilde{p} + \widehat{\boldsymbol{\varrho}}_{_T}{}^{-1}\,\nabla A\,\widetilde{p}\\ \widetilde{\sigma}\,(\mathbf{x},\omega) &= \varrho_{\text{ref}}\,\omega^2\left(\frac{1}{\mathcal{K}_{\text{ref}}} - \frac{1}{\mathcal{K}_{_T}}\right)\widetilde{p}\end{aligned} \tag{19}$$

In all the simulations, the reference density and compressibility are those of the hosting medium in the asymptotic conditions, $\varrho_{_\infty}$ and $\mathcal{K}_{_\infty}$. The obstacle considered is a cylindrical object of infinite extension, so the domain of calculation can be reduced to

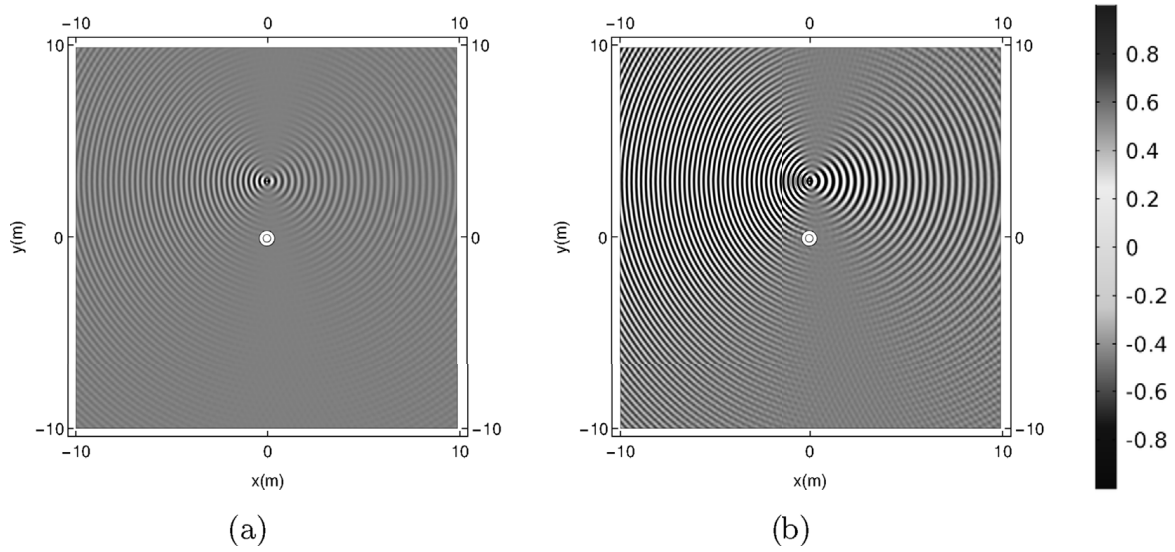

Fig. 4. Field patterns of the $\mathcal{O}(M_{_\infty}^2)$ neglected convective terms for $k_{_R} = 4$ (normalised grey levels) and $M_{_\infty} = 0.1$ in (a) and $M_{_\infty} = 0.2$ in (b).

Table 1
Locations of the acoustic source considered in the simulations. Coordinates are referred to a frame of reference with origin on the center of the cylinder. Units are expressed in meters.

position Id	relative location	coordinates
A	above	$\mathbf{x}_{_S} = (0, 3)$
B	above and upwind	$\mathbf{x}_{_S} = (-1.5\sqrt{2}, 1.5\sqrt{2})$
C	aligned upwind	$\mathbf{x}_{_S} = (-3, 0)$
D	aligned downwind	$\mathbf{x}_{_S} = (3, 0)$

a two–dimensional space. Following Fig. 3, we call Ω_h the hosting domain, where the acoustic propagation in a moving medium is described by

$$-i\omega\frac{\rho_0}{c_0^2}\left(i\omega\widetilde{\varphi}+\mathrm{v}_0\cdot\nabla\widetilde{\varphi}\right)+\nabla\cdot\left(\rho_0\nabla\widetilde{\varphi}-\frac{\rho_0}{c_0^2}\left(i\omega\widetilde{\varphi}+\mathbf{v}_0\cdot\nabla\widetilde{\varphi}\right)\mathbf{v}_0\right)=0 \tag{20}$$

The cylinder of radius $R_1=0.2$ m, centered in $\mathbf{x}_c=(0,0)$, is surrounded by a circular cloaking of radius $R_2=0.4$ m. An isotropic acoustic point source S is located in $\mathbf{x}_s=(\mathbf{x}_s,y_s)$ and is fixed with respect to the cylinder and the cloak. Γ denotes the boundary of the circle and Γ_c the interface between the hosting and the cloak domain Ω_c.

Numerical simulations are carried out in frequency domain using the finite element method. Fourier transforming Eq. (12), the equation governing the propagation of the acoustic perturbation in Ω_h is

$$-i\omega\frac{\rho_0}{c_0^2}\left(i\omega\widetilde{\varphi}+\mathbf{v}_0\cdot\nabla\widetilde{\varphi}\right)+\nabla\cdot\left(\rho_0\nabla\widetilde{\varphi}-\frac{\rho_0}{c_0^2}\left(i\omega\widetilde{\varphi}+\mathbf{v}_0\cdot\nabla\widetilde{\varphi}\right)\mathbf{v}_0\right)=0 \tag{21}$$

The applicability of the Taylor transformation requires that $\mathbf{v}_0=\nabla\Phi$ with $\nabla^2\Phi(\mathbf{x})=0$ with impermeability boundary conditions on $\Gamma(\mathbf{x})$. Equations (17) and (21) are coupled, solving the first in Ω_c (no aerodynamic velocity is allowed inside the cloak domain) and the latter in Ω_h. The solution of Eq. (21) is calculated for the statically designed and the convective corrected cloaks, and compared with the primary field obtained when no obstacles are present in the field. The continuity of the acoustic field at the media interface must be ensured, such that both pressure and particles' normal acceleration are continuous at the interface Γ_c,

$$\widetilde{p}_c=\widetilde{p}_h,\quad \boldsymbol{\varrho}_T^{-1}\nabla\widetilde{p}\cdot\mathbf{n}=j\omega\mathbf{v}_h\cdot\mathbf{n} \tag{22}$$

Non–reflecting conditions are applied at the external boundary of the computational domain to simulate the radiation of the disturbance to the far field. To confirm the broadband efficiency of metadevices designed within the proposed theoretical framework, the analysis is performed in the reduced frequency range $1\le k_R\le 4$ with $k_R=k_0R_1$. All the simulations are repeated for different values of Mach number of the background aerodynamic flow in the range $0<M_\infty<0.35$, compatible with the

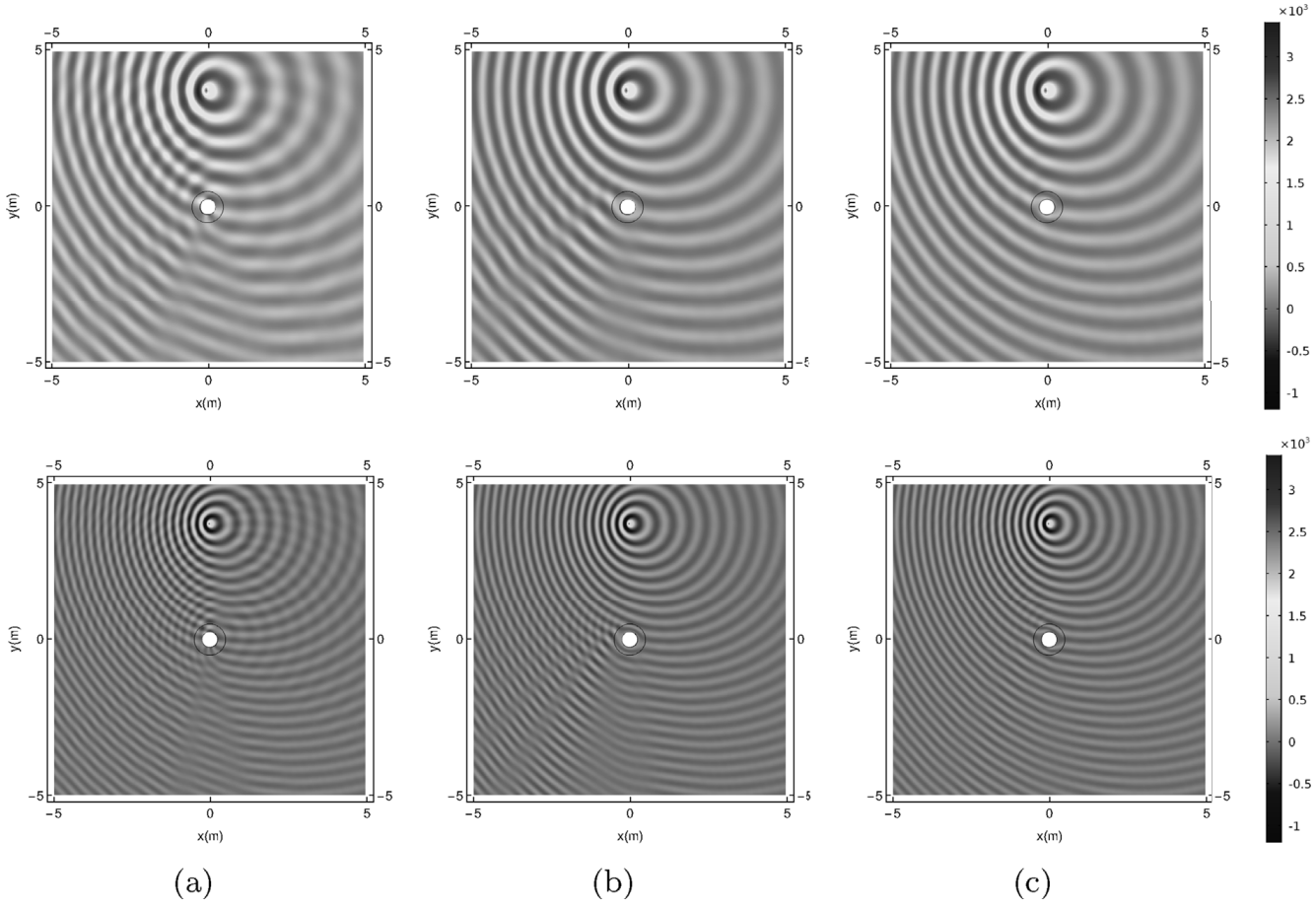

Fig. 5. Field visualisation at M = 0.35 for $k_R=2,4$ (top to bottom), source position *A*. Column (a) refers to the naked obstacle, column (b) to the static cloak and column (c) to the convective cloak.

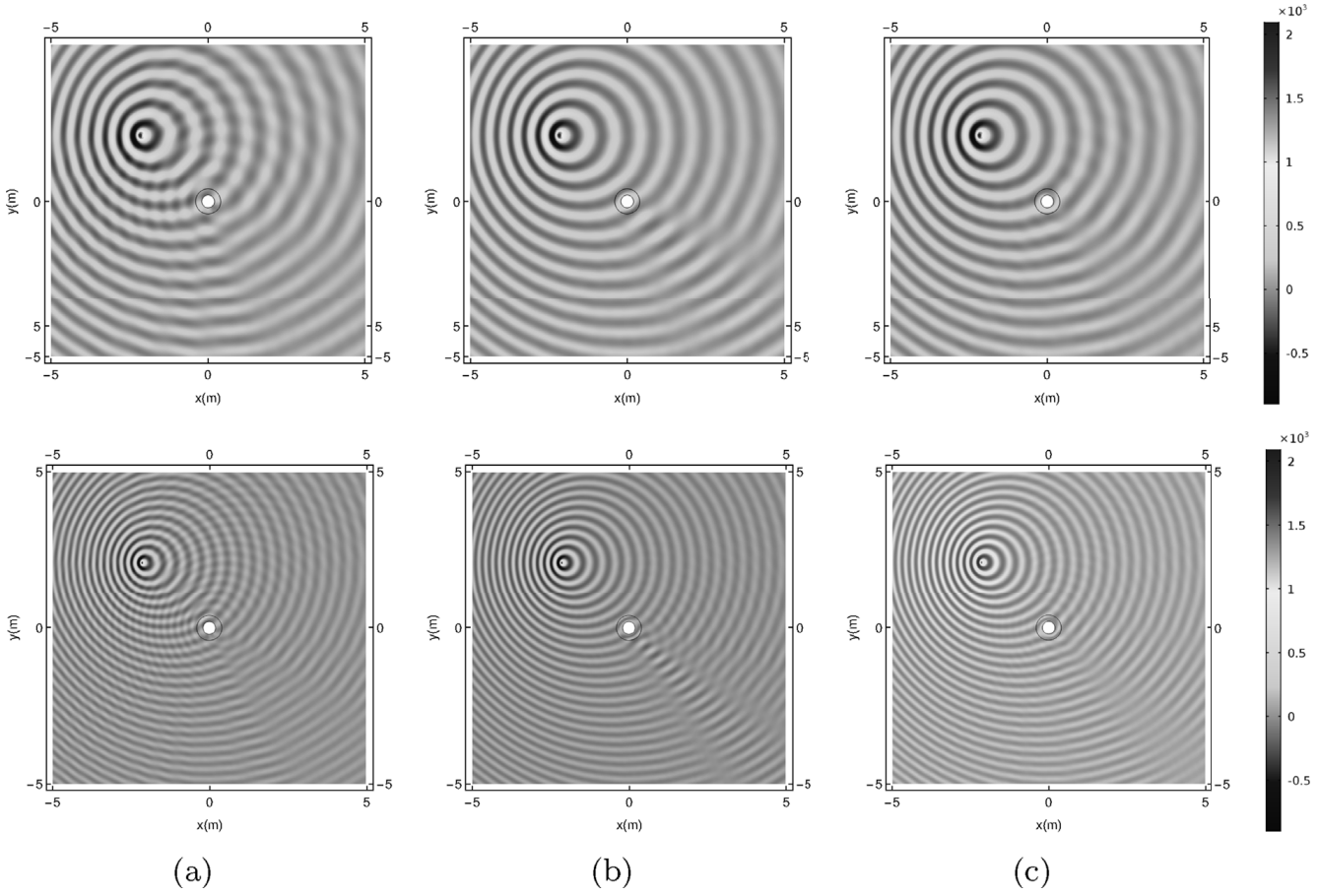

Fig. 6. Field visualisation at M = 0.35 for $k_R = 2, 4$ (top to bottom), source position *B*. Column (a) refers to the naked obstacle, column (b) to the static cloak and column (c) to the convective cloak.

approach and take off speeds of a commercial aircraft. In order to understand and interpret properly the results of the numerical simulations, it is first necessary to analyse with some detail the effect of the low–speed approximation underlying the Taylor transform.

Before showing the results of numerical simulations, in the following subsection we present an analysis of the terms neglected in the $\mathcal{O}(M_\infty)$ approximation of the governing equation. Their form is (see, *e.g.*, Vaidya [23])

$$\epsilon = \mathbf{v}_0 \cdot \nabla \left(\mathbf{v}_0 \cdot \nabla \varphi \right) + \frac{1}{2} \nabla \varphi \cdot \nabla |\mathbf{v}_0|^2 + (\gamma - 1) \left(\frac{\partial}{\partial t} + \mathbf{v}_0 \cdot \nabla \right) \varphi \, \nabla \cdot \mathbf{v}_0 + \frac{\gamma - 1}{2} (c_0^2 - c_\infty^2) \nabla^2 \varphi \tag{23}$$

where γ is the ratio of specific heats. A detailed dimensional analysis of each term of the error ϵ can be found in Mancini et al. [24]. Here, we limit our attention to regions of Ω_h where Eq. (23) can be significantly simplified. Let's assume that the local flow velocity is the superposition of a perturbation $\mathbf{u}$ on the asymptotic free–stream, $\mathbf{v}_0 = \mathbf{v}_\infty + \mathbf{u}$, and that the source is located at a distance from the obstacle such that $\|\mathbf{u}\| \ll \left\| \mathbf{v}_\infty \right\|$. In this conditions, and assuming the asymptotic free–stream aligned with the $x-$axis, Eq. (23) reduces to

$$\epsilon = \mathbf{v}_\infty^2 \frac{\partial^2 \varphi}{\partial \mathbf{x}^2} \quad . \tag{24}$$

Fig. 4 shows the structure of the contribution of ϵ to the primary field induced by the source. The evident dipole–like propagation pattern clearly indicates that privileged relative positions between the emitting source and the scattering object exist, and the maximum efficiency loss of the Taylor–corrected device is expected when the acoustic source is aligned along the free–stream direction.

Indeed, the $\mathcal{O}(M_\infty)$ convective correction neglects this term, thus lacking the capability to recover its negative effect on the metamaterial response. In the FEM simulations that are reported in the following, four different locations of the source are analysed in order to validate numerically the effect of the neglected terms. Specifically, the source is placed in the sectors corresponding to the least and maximum radiation of ϵ (positions *A* and *D*, respectively), in the intermediate position *B*, and in the sector corresponding to a high radiation level of ϵ and a positive Doppler shift (position *C*). All the locations are summarised in Table 1.

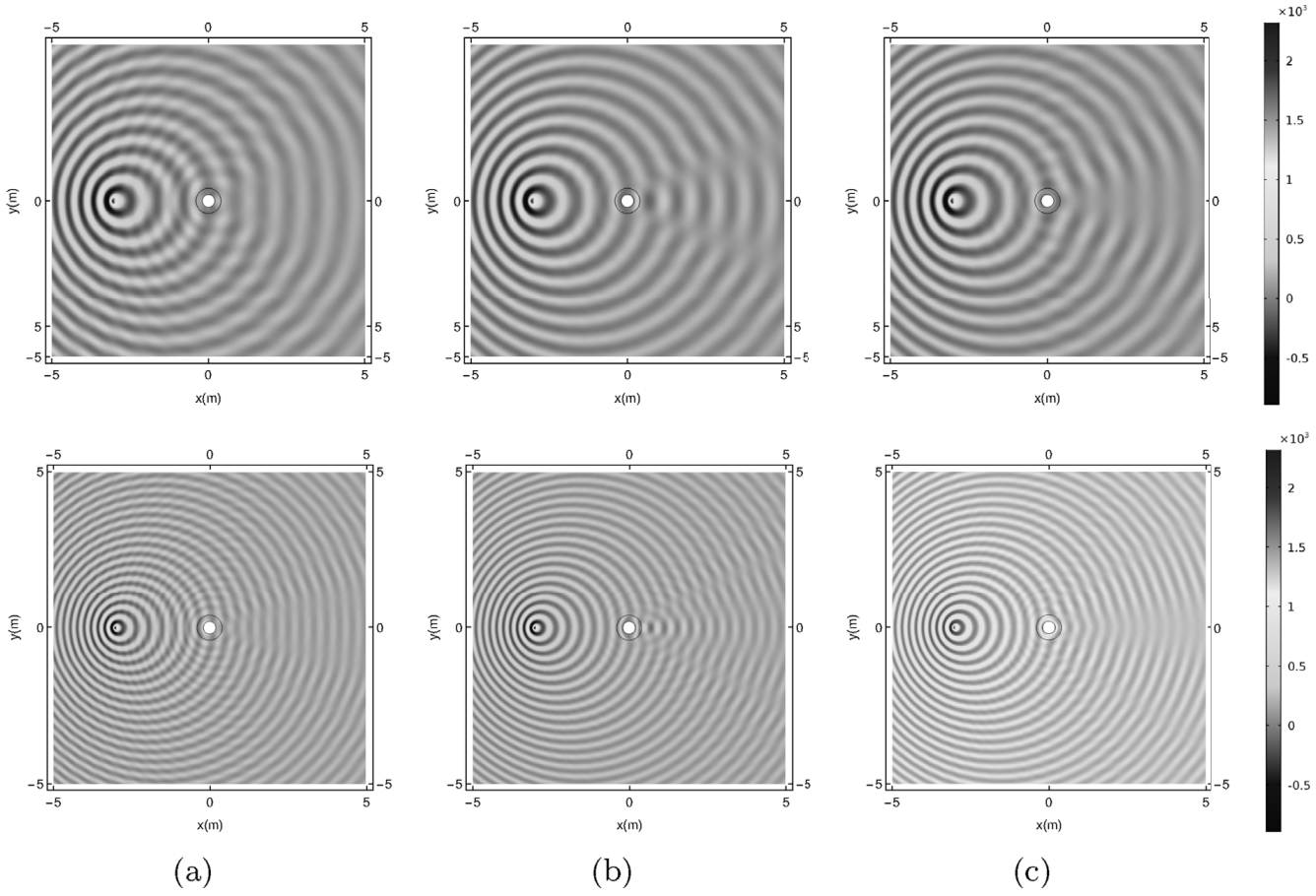

Fig. 7. Field visualisation at M = 0.35 for $k_R = 2, 4$ (top to bottom), source position *C*. Column (a) refers to the naked obstacle, column (b) to the static cloak and column (c) to the convective cloak.

The first set of results corresponds to position *A*. Fig. 5 compares the real part of the total pressure field for the static and corrected cloaks with the scattering pattern induced by the untreated obstacle at $k_R = 2, 4$. The recovery effect of the convective correction proposed is evident at both frequencies, confirming that the broadband behaviour typical of an IC device is preserved by the correction. When the source is located in the sectors of high ϵ intensity the correction loses part of its efficiency. Figs. 6–8 show how the corrected device cannot recover completely the scattering cancellation, even if its performance is always better than that obtained by the uncorrected metamaterial. This effect can be better observed in Figs. 9–16, where the directivity plots of the insertion loss I_L are presented for different values of M_∞. The loss index I_L is defined as

$$\mathrm{I_L} = 20 \log_{10} \left(\frac{p_i}{p_t} \right), \tag{25}$$

were p_i is the incident pressure field induced by the isolated source, and p_t is the total pressure field occurring in presence of the treated or un–treated obstacle. The I_L is evaluated at a circle of microphones located at $R_{\mathrm{mic}} = 5R_2$, for $k_R = 2$ and $k_R = 4$. Coherently with the underlying $\mathcal{O}(M_\infty)$ approximation, for all the source positions, the performance of the corrected cloak reduces when the Mach number rises. When the source is located at positions *B*, *C*, and *D* the corrected metamaterial outperforms the static one along the entire circle of monitoring points, with a residual shadow of intensity comparable to that of the untreated object, but with a limited polar extension. In the same region, the static metamaterial causes a perturbation much stronger than the one observable for the naked scatterer.

These considerations are further confirmed by the analysis of the scattering cross section, defined as (see *e.g.,* Iemma and Burghignoli [20])

$$\sigma_{cs} = \frac{1}{2\pi \mathrm{r_{mic}}} \int_0^{2\pi} \left(\frac{\widetilde{p}_s^{\,\mathrm{rms}}}{\widetilde{p}_i^{\,\mathrm{rms}}} \right)^2 d\theta = \frac{1}{2\pi \mathrm{r_{mic}}} \int_0^{2\pi} \frac{|p_s|^2}{|p_i|^2} d\theta \tag{26}$$

where p_s is the scattered pressure, $p_t - p_i$. The scattering cross section σ is calculated for positions *A* and *C*. Fig. 17 shows the value of σ_{cs} for $0 \leq M_\infty \leq 0.35$ and source on position *A*. The almost complete recovery of the efficiency of the matamaterial device extends over the entire range of M_∞ analysed. This result is of particular interest in relation to aeronautical applications, being the existing corrections limited to much lower values, incompatible with realistic operating conditions

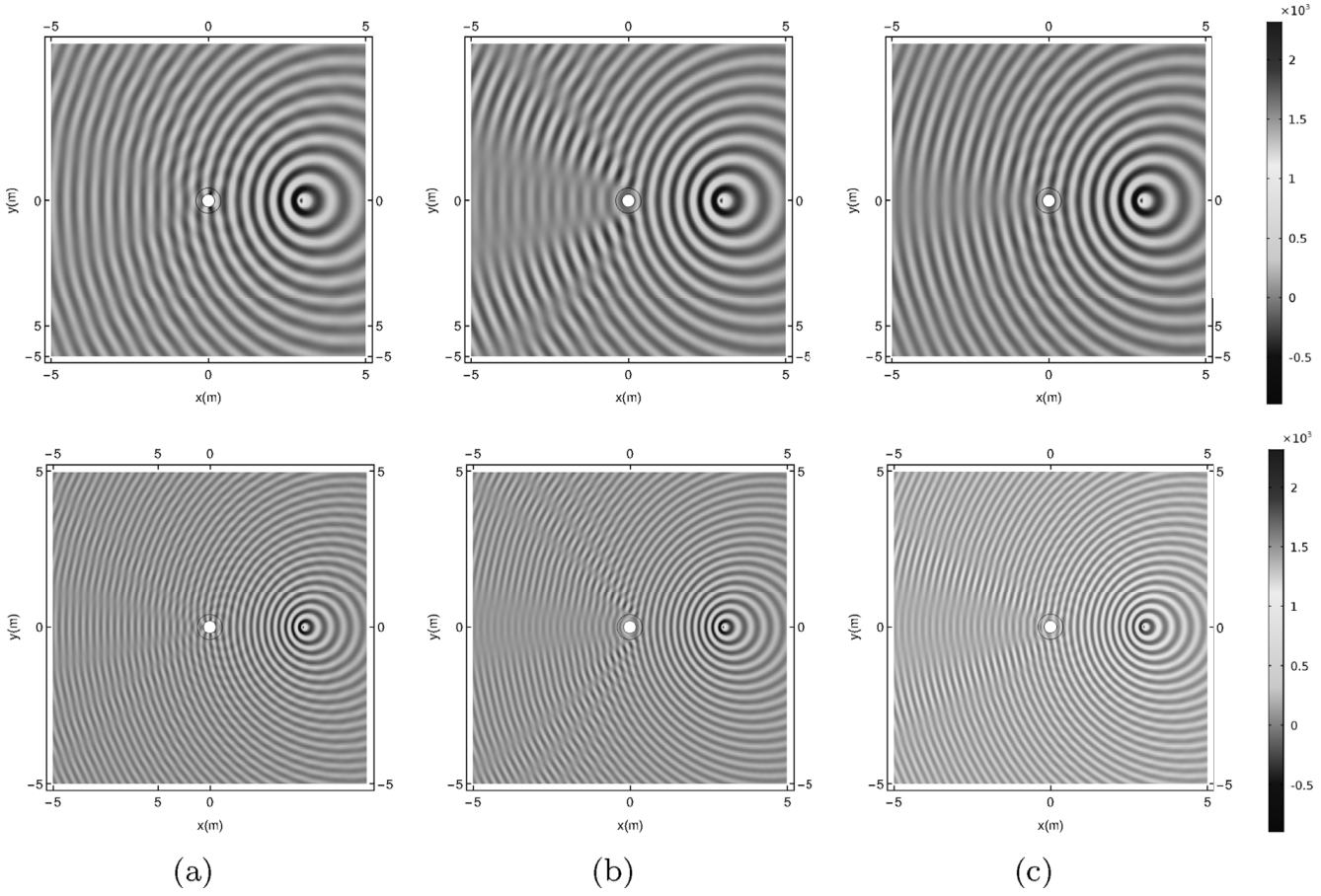

Fig. 8. Field visualisation at M = 0.35 for $k_R = 2, 4$ (top to bottom), source position *D*. Column (a) refers to the naked obstacle, column (b) to the static cloak and column (c) to the convective cloak.

of an aircraft (see Huang et al. [10]). Furthermore, it is interesting to notice how the response of the uncorrected material deteriorates at higher speeds, inducing a perturbation even worse than that of an untreated object beyond a certain value of M_∞.

The results obtained for the source in position *C* are depicted in Fig. 18. The performance loss is evident at all the frequencies analysed. Corrected and static device both produce a scattering field higher than that of the naked obstacle beyond a critical value of M_∞, which is always higher for the corrected one.

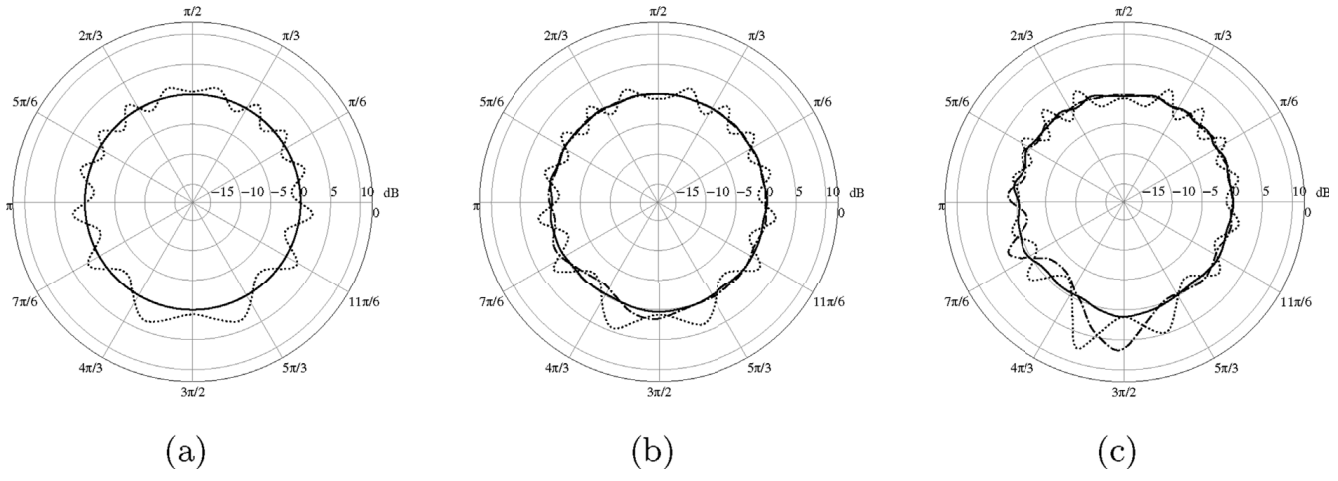

Fig. 9. Insertion Loss directivity plot (dB), source in position *A*, $k_R = 2$, dotted line for naked cylinder, dashed and solid lines respectively for static and convective designs. (a) $M_\infty = 0$, (b) $M_\infty = 0.2$, (c) $M_\infty = 0.35$.

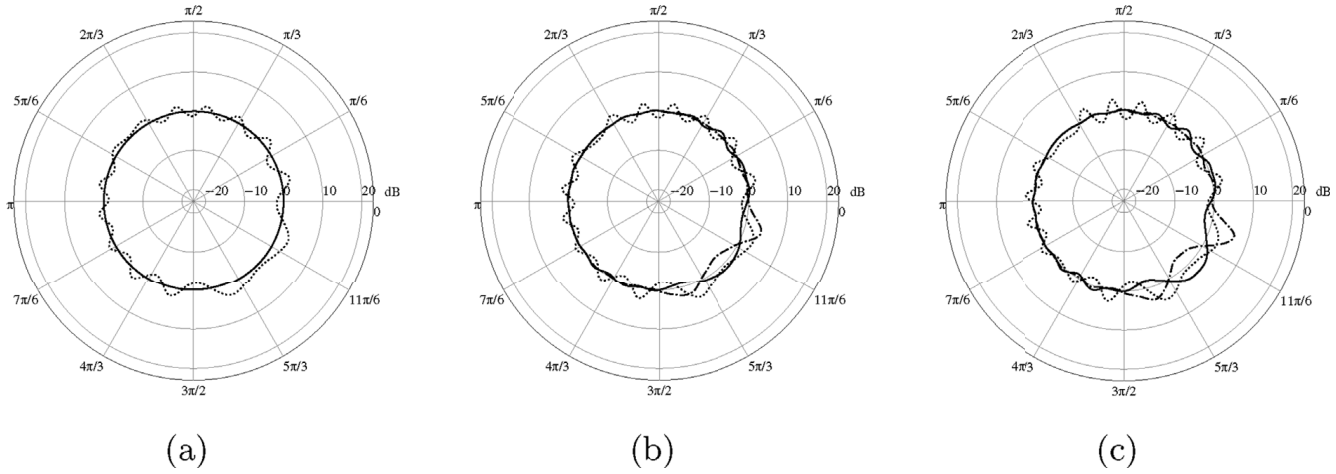

Fig. 10. Insertion Loss directivity plot (dB), source in position B, $k_R = 2$, dotted line for naked cylinder, dashed and solid lines respectively for static and convective designs. (a) $M_\infty = 0$, (b) $M_\infty = 0.2$, (c) $M_\infty = 0.35$.

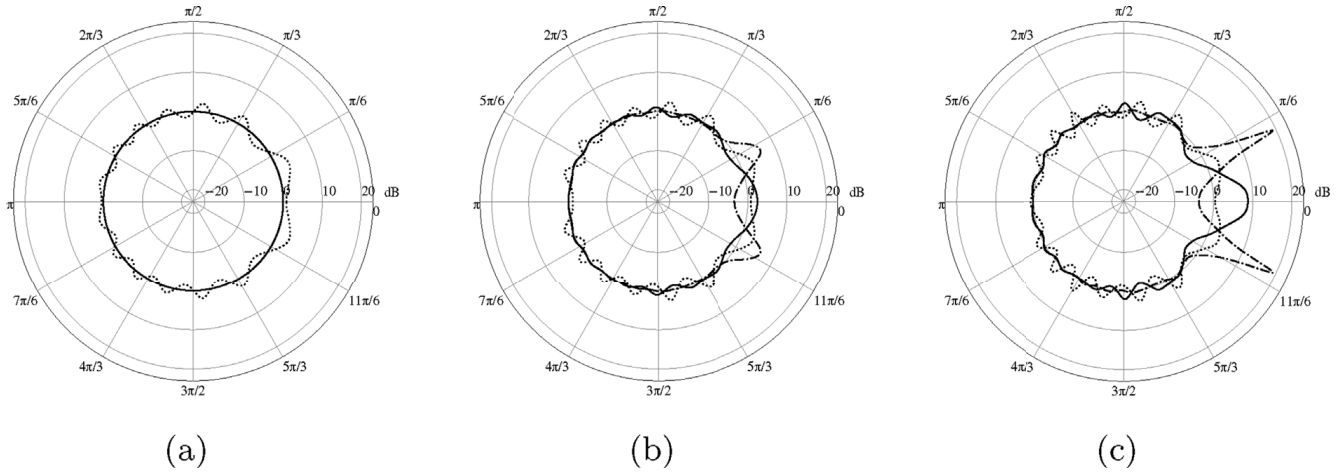

Fig. 11. Insertion Loss directivity plot (dB), source in position C, $k_R = 2$, dotted line for naked cylinder, dashed and solid lines respectively for static and convective designs. (a) $M_\infty = 0$, (b) $M_\infty = 0.2$, (c) $M_\infty = 0.35$.

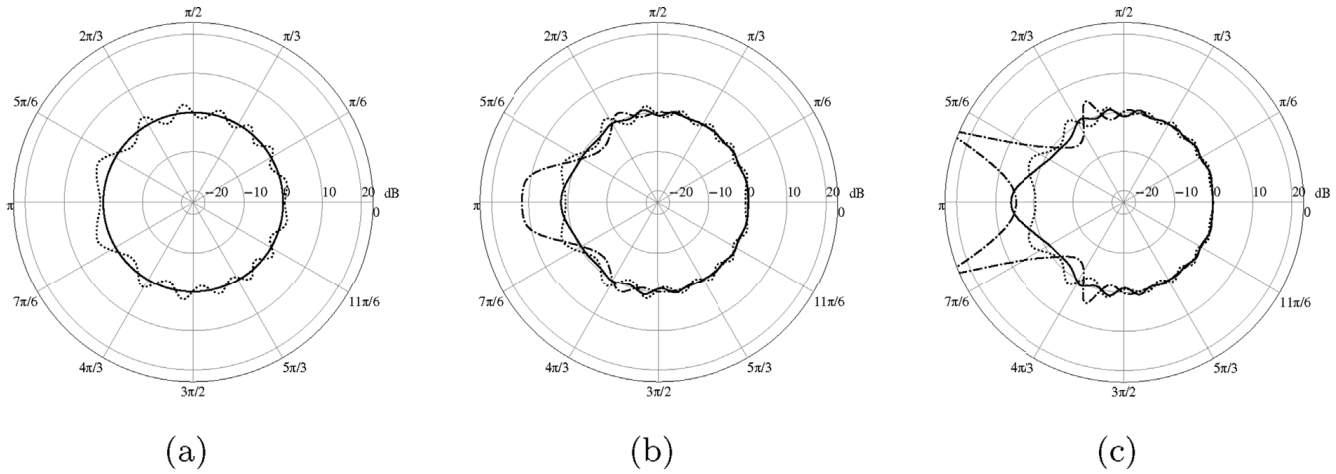

Fig. 12. Insertion Loss directivity plot (dB), source in position D, $k_R = 2$, dotted line for naked cylinder, dashed and solid lines respectively for static and convective designs. (a) $M_\infty = 0$, (b) $M_\infty = 0.2$, (c) $M_\infty = 0.35$.

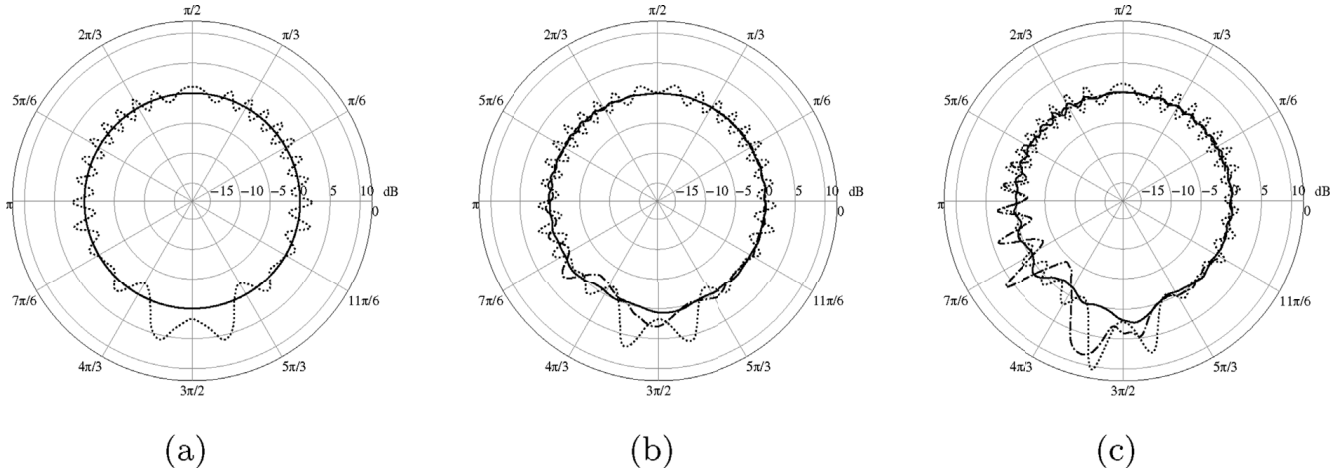

Fig. 13. Insertion Loss directivity plot (dB), source in position *A*, $k_R = 4$, dotted line for naked cylinder, dashed and solid lines respectively for static and convective designs. (a) $M_\infty = 0$, (b) $M_\infty = 0.2$, (c) $M_\infty = 0.35$.

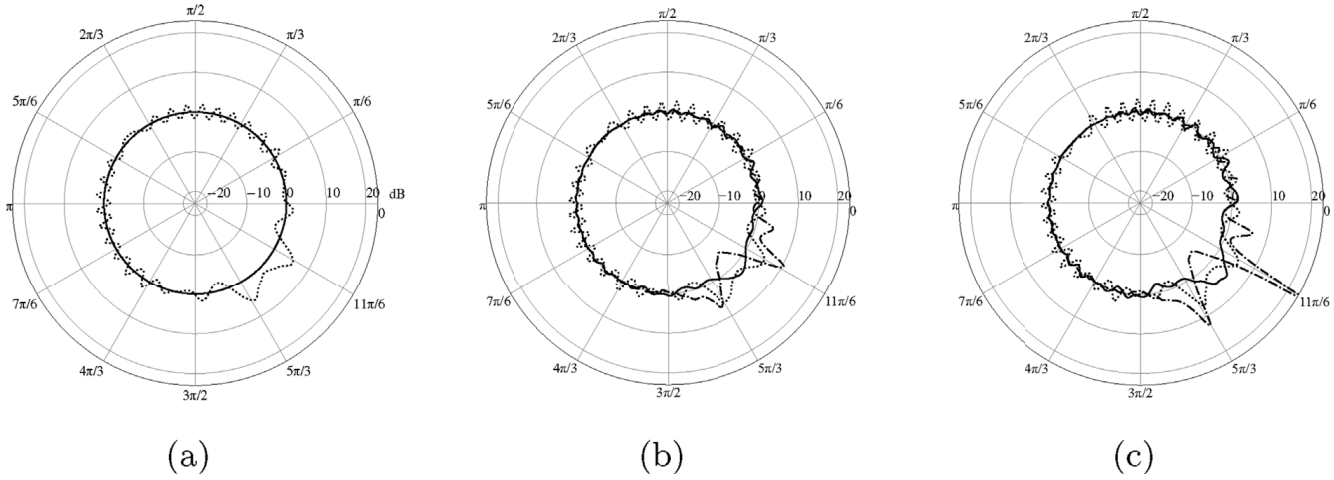

Fig. 14. Insertion Loss directivity plot (dB), source in position *B*, $k_R = 4$, dotted line for naked cylinder, dashed and solid lines respectively for static and convective designs. (a) $M_\infty = 0$, (b) $M_\infty = 0.2$, (c) $M_\infty = 0.35$.

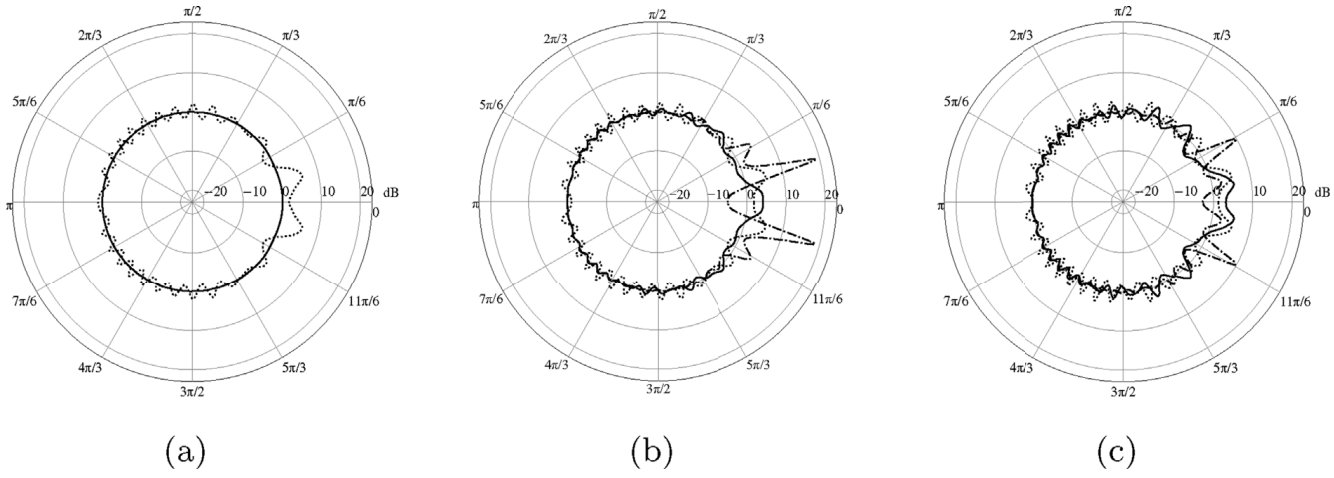

Fig. 15. Insertion Loss directivity plot (dB), source in position *C*, $k_R = 4$, dotted line for naked cylinder, dashed and solid lines respectively for static and convective designs. (a) $M_\infty = 0$, (b) $M_\infty = 0.2$, (c) $M_\infty = 0.35$.

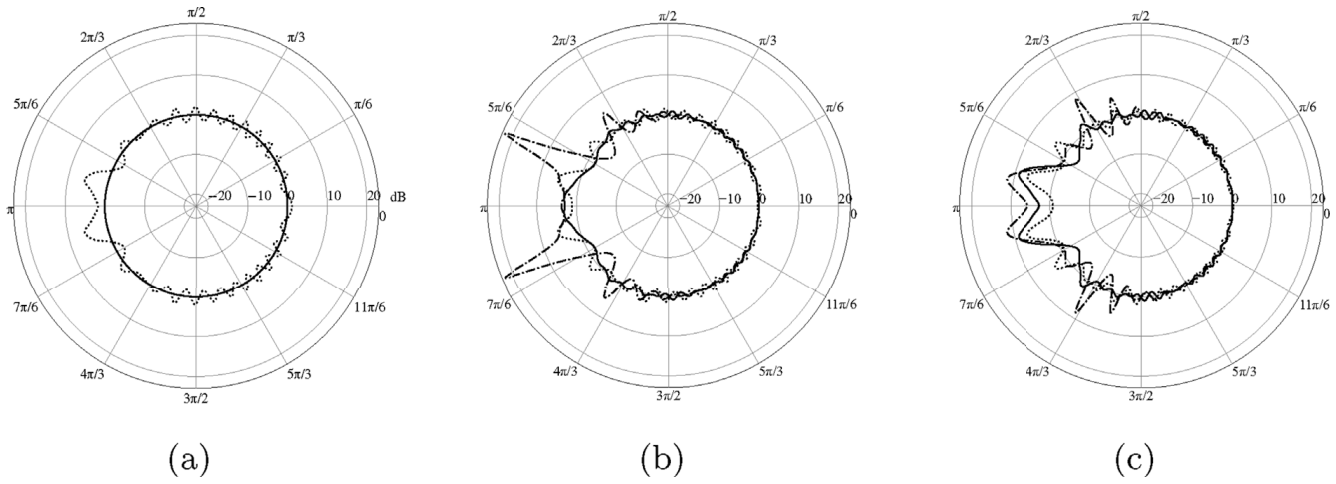

Fig. 16. Insertion Loss directivity plot (dB), source in position D, $k_R = 4$, dotted line for naked cylinder, dashed and solid lines respectively for static and convective designs. (a) $M_\infty = 0$, (b) $M_\infty = 0.2$, (c) $M_\infty = 0.35$.

In summary, the analytical and numerical assessment of the proposed convective correction has revealed that the $\mathcal{O}(M_\infty)$ approximation on the basis of the Taylor transform makes the efficiency of the resulting device strongly dependent on the position of the source. Nevertheless, in the most favourable cases the recovery of the expected response is almost complete, making the method appealing for all those applications compatible with the best relative positioning of sources and obstacles.

Finally, some considerations deserve to be done about the chances to actually realise the proposed convective design. Although the present work is focused on the theoretical development and the numerical validation of the fundamental idea, and any attempt to define in details the manufacturing of the corrected device is premature and beyond the scope of the paper, it could be of some interest at least identifying potential development strategies aiming at the fabrication of such a material. Looking back at Eqs. (15)–(18), it can be seen that the convective correction proposed induces two effects: *i*) an exponential correction factor of the density tensor and the compressibility coefficient in the frequency domain, corresponding to a time–shift (in principle anti–causal) in the time domain; *ii*) a distribution of equivalent sources depending on the perturbation pressure and its gradient. For a periodic signal, the first effect is equivalent to a suitable phase change depending only on the local speed of the potential flow that would be present in Ω_c around the naked obstacle impinged by the stream. The possibility to induce a non–uniform phase shift is one of the most active research topics in the field of acoustic metamaterial and metasurfaces (see Ref. [25] for an extensive review). The substantial literature available covers a large number of solutions and concepts, validated and assessed through numerical simulations and experiments. Some of these solutions are particularly appealing for aeronautical applications, being characterised by overall dimensions and a specific weight compatible with the strict design constraints (see, *e.g.,* [26–28]). The second effect is more technologically challenging, being related to the possibility of inducing a point–wise acoustic excitation distributed in Ω_c depending on the local value of the total pressure and its gradient. This requires the establishment of an active system capable to locally react to the acoustic field. There are several approaches currently available in the literature that could be the starting point for the development of this kind of active materials. Among others, we'd like to

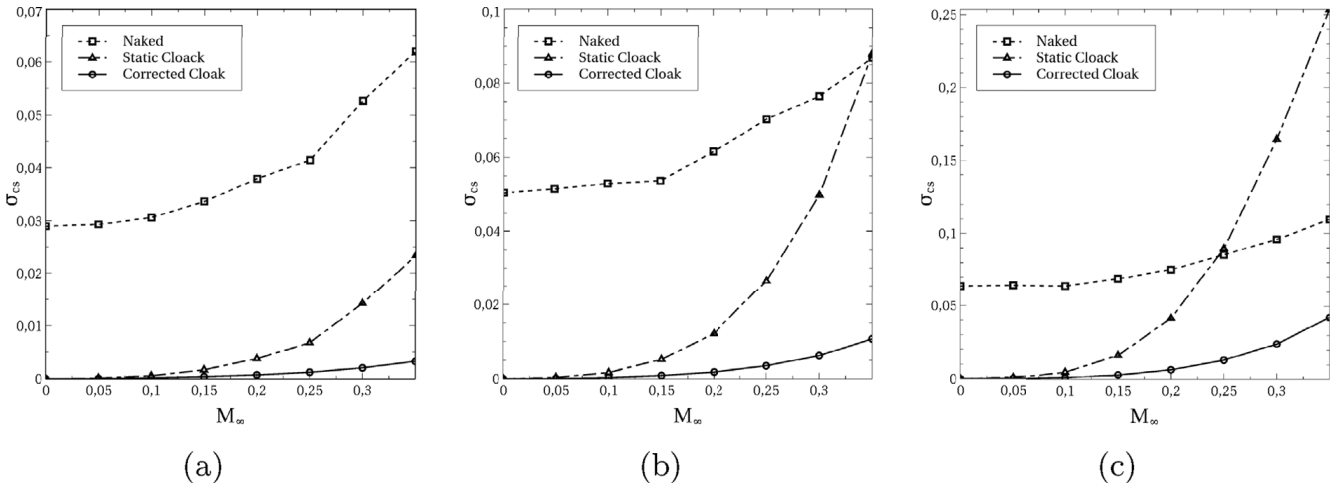

Fig. 17. Scattering Cross Section vs Mach number at $k_R = 1$ (a), $k_R = 2$ (b), and $k_R = 4$ (c). Source in position A.

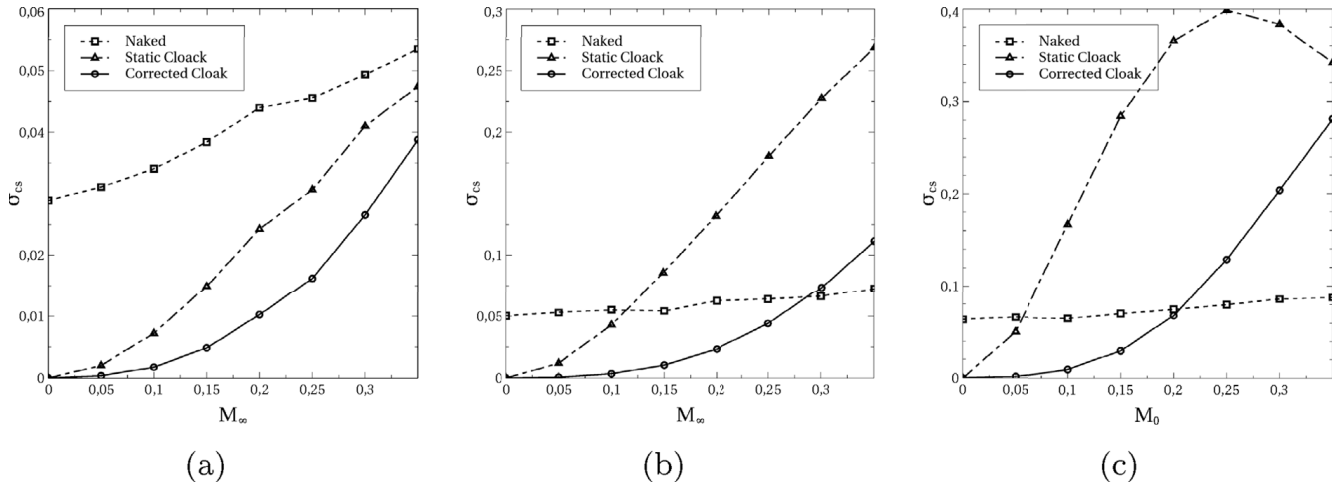

Fig. 18. Scattering Cross Section vs Mach number at $k_R = 1$ (a), $k_R = 2$ (b), and $k_R = 4$ (c). Source in position C.

mention two interesting approaches. On one side, the remarkable potential of the magnetorheological fluids, capable to change significantly their mechanical properties almost instantaneously under the action of a variable magnetic field (see, *e.g.,* [29]), and on the other side the approach sketched in Ref. [30], where a high energy laser beam is focused to heat a very small volume of fluid creating a very small plasma zone that, rapidly expanding, generates an omni-directional pressure wave that propagates at the isentropic speed of sound, *i.e.* a monopole (quasi) point source. The technology readiness level of both these techniques is very low ($TRL \leq 3$), so it is premature to speculate on the impact that this device would have on aspects that are key in aeronautical applications, such as weight penalties, production and service costs, reliability. However, it is important to stress one more time that the aspects related to realisability and manufacturing are secondary in the context of the present work, which focuses on the analysis of the applicability and the effectiveness of the method to existing metamaterial static design, taking advantage of an analytical instrument widely used by the aeroacoustic community easily integrable in the available analysis tools.

5. Concluding remarks

A new formulation for the design of metamaterial/metafluid–based devices operating in a flow has been presented. The method is based on the application of the Taylor transformation to the equation governing the response of a statically designed metamaterial. The use of the Taylor transformation ensures that the non-uniformity of the background flow is taken into account, under the assumption of potential aerodynamics at low Mach number. The Taylor transformation is used to derive the mechanical properties of an equivalent aeroacoustic metafluid capable to attain the target response in presence of a background flow. The formulation presented is independent on the specific method used for the static design of the metamaterial and can be applied, in principle, to any existing metafluid. The method has been validated through numerical simulations on the aeroacoustic cloaking of a moving circular cylinder of infinite extension, impinged by the acoustic perturbation generated by a co–moving monopole. The configuration analysed mimics a situation typical of aeronautical applications, where the noise sources (engines, landing gears, high–lift devices…) and the scattering obstacles (wings, fuselage, empennages…) are rigidly connected to each other and at close distance, making the common assumption of planar wave fronts fail.

The effectiveness of the metafluid cloak designed with the proposed method has been assessed through numerical simulation using the FEM. The asymptotic Mach numbers of the background flow has been tested up to $M = 0.35$, much higher than what available so far in the literature so far and compatible with the take–off and landing procedures of a commercial aircraft. Although the static metamaterial is designed to have an isotropic response when operating in a quiescent medium, independent on the relative position of the source and the scatterer, the numerical results show that the corrected device exhibits a not negligible dependence of the response on the spatial configuration. This behaviour has been explained analytically as the effect of the terms neglected in the $\boldsymbol{\mathcal{O}}(M_\infty)$ convective correction. The analytical demonstration has been extensively verified numerically, showing that the worst operating conditions are those where the source and the scatterer are aligned along the direction of motion. On the other hand, when the alignment of source and object is orthogonal to their velocity vector, the recovery of the metamaterial response is almost complete, making the approach extremely appealing for all the engineering applications where the relative position of the noise sources is compatible with this favourable layout. This is the case of most of the aeronautical applications mentioned above. In addition, the broadband meta behaviour of the designed device has been confirmed in the reduced frequency range $1 \leq k_0 R \leq 4$, demonstrating that the proposed correction preserves the broadband response of the original static design. The proposed correction implies that in practical applications an aeroacoustic metafluid should exhibit active properties to reproduce the distributed sources that mimic the convection effects within Ω_c. Although this specific aspect induces challenging technology requirements, some recent advancements in the experimental generation of acoustic source through high–energy thermodynamic excitation or magnetorheological fluids could be the key to the realization of a new generation of active materials.

Acknowledgements

The research is supported by the European Commission through project AERIALIST (AdvancEd aicRaft-noIse-AlLeviation devIceS using meTamaterials), H2020–MG–1.4–2016–2017, project no. 723367.

References

[1] S.A. Cummer, D. Schurig, One path to acoustic cloaking, New J. Phys. 9 (3) (2007) 45. https://doi.org/10.1088/1367-2630/9/3/045.
[2] R.M. Walser, Electromagnetic metamaterials, Proc. SPIE 4467 (2001), https://doi.org/10.1117/12.432921 4467–15.
[3] J.B. Pendry, D. Schurig, D.R. Smith, Controlling electromagnetic fields, Science 312 (5781) (2006) 1780–1782, https://doi.org/10.1126/science.1125907.
[4] U. Leonhardt, Optical conformal mapping, Science 312 (5781) (2006) 1777–1780, https://doi.org/10.1126/science.1126493.
[5] L.W. Cai, J. Sánchez-Dehesa, Analysis of cummer–schurig acoustic cloaking, New J. Phys. 9 (12) (2007) 450. https://doi.org/10.1088/1367-2630/9/12/450.
[6] D. Torrent, J. Sánchez-Dehesa, Broadband acoustic cloaks based on the homogenization of layered materials, Wave Motion 48 (6) (2011) 497–504 special Issue on Cloaking of Wave Motion, https://doi.org/10.1016/j.wavemoti.2011.04.008.
[7] A. Climente, D. Torrent, J. Sánchez-Dehesa, Sound focusing by gradient index sonic lenses, Appl. Phys. Lett. 97 (10) (2010) 104103, https://doi.org/10.1063/1.3488349.
[8] A.N. Norris, Acoustic cloaking theory, Proc. Roy. Soc. Lond. A: Math., Phys. Eng. Sci. 464 (2097) (2008) 2411–2434, https://doi.org/10.1098/rspa.2008.0076.
[9] A.N. Norris, Acoustic metafluids, J. Acoust. Soc. Am. 125 (2) (2009) 839–849, https://doi.org/10.1121/1.3050288.
[10] X. Huang, S. Zhong, O. Stalnov, Analysis of scattering from an acoustic cloak in a moving fluid, J. Acoust. Soc. Am. 135 (5) (2014) 2571–2580, https://doi.org/10.1121/1.4869815.
[11] U. Iemma, Theoretical and numerical modeling of acoustic metamaterials for aeroacoustic applications, Aerospace 3 (2) (2016) 15, https://doi.org/10.3390/aerospace3020015.
[12] X. Huang, S. Zhong, X. Liu, Acoustic invisibility in turbulent fluids by optimised cloaking, J. Fluid Mech. 749 (2014) 460–477, https://doi.org/10.1017/jfm.2014.250.
[13] C. García-Meca, S. Carloni, C. Barceló, G. Jannes, J. Sánchez-Dehesa, A. Martínez, Analogue transformations in physics and their application to acoustics, Sci. Rep. 3 (2013) 2009, https://doi.org/10.1038/srep02009.
[14] C. García-Meca, S. Carloni, C. Barceló, G. Jannes, J. Sánchez-Dehesa, A. Martinez, Supplementary information: analogue transformations in physics and their application to acoustics, Sci. Rep. 30 (2009), https://doi.org/10.1038/srep02009.
[15] C. García-Meca, S. Carloni, C. Barceló, G. Jannes, J. Sánchez-Dehesa, A. Martínez, Space-time transformation acoustics, Wave Motion 51 (5) (2014) 785–797. https://doi.org/10.1016/j.wavemoti.2014.01.008.
[16] C. García-Meca, S. Carloni, C. Barceló, G. Jannes, J. Sánchez-Dehesa, A. Martínez, Analogue transformation acoustics and the compression of spacetime, Photon. Nanostruct. - Fund. Appl. 4 (4) (2014) 312–318. https://doi.org/10.1016/j.photonics.2014.05.001.
[17] U. Iemma, G. Palma, Analogue transformation acoustics in aeronautics, in: 46th International Congress and Exposition on Noise Control Engineering, Inter-noise 2017, 2017.
[18] U. Iemma, G. Palma, On the use of the analogue transformation acoustics in aeroacoustics, Math. Probl Eng. 2017 (2017) 16 article ID 8981731, https://doi.org/10.1155/2017/8981731.
[19] H. Ryoo, W. Jeon, Effect of compressibility and non-uniformity in flow on the scattering pattern of acoustic cloak, Sci. Rep. 7 (1) (2017) 2125, https://doi.org/10.1038/s41598-017-02143-y.
[20] U. Iemma, L. Burghignoli, An integral equation approach to acoustic cloaking, J. Sound Vib. 331 (21) (2012) 4629–4643. https://doi.org/10.1016/j.jsv.2012.04.032.
[21] K. Taylor, A transformation of the acoustic equation with implications for wind-tunnel and low-speed flight tests, Proc. Roy. Soc. Lond. A: Math., Phys. Eng. Sci. 363 (1713) (1978) 271–281, https://doi.org/10.1098/rspa.1978.0168.
[22] M.E. Gurtin, An Introduction to Continuum Mechanics, Academic Press, New York, 1981.
[23] P.G. Vaidya, Propagation of sound in flows containing mean flow gradients, in: 7th AIAA Aeroacoustics Conference, 1981, pp. 1981–1987, https://doi.org/10.2514/6.1981-1987.
[24] S. Mancini, R.J. Astley, S. Sinayoko, G. Gabard, M. Tournour, An integral formulation for wave propagation on weakly non-uniform potential flows, J. Sound Vib. 385 (2016) 184–201, https://doi.org/10.1016/j.jsv.2016.08.025, arXiv:1509.06426.
[25] G. Palma, H. Mao, L. Burghignoli, P. Gransson, U. Iemma, Acoustic metamaterials in aeronautics, Appl. Sci. 8 (6) (2018), https://doi.org/10.3390/app8060971, http://www.mdpi.com/2076-3417/8/6/971.
[26] Y. Li, X. Jiang, R.-q. Li, B. Liang, X.-y. Zou, L.-l. Yin, J.-c. Cheng, Experimental realization of full control of reflected waves with subwavelength acoustic metasurfaces, Phys. Rev. Appl. 2 (2014) 064002, https://doi.org/10.1103/PhysRevApplied.2.064002, https://link.aps.org/doi/10.1103/PhysRevApplied.2.064002.
[27] X. Jiang, B. Liang, X.-y. Zou, J. Yang, L.-l. Yin, J. Yang, J.-c. Cheng, Acoustic one-way metasurfaces: asymmetric phase modulation of sound by subwavelength layer, Sci. Rep. 6 (2016) 28023, https://doi.org/10.1038/srep28023.
[28] Y.-F. Zhu, X.-Y. Zou, R.-Q. Li, X. Jiang, J. Tu, B. Liang, J.-C. Cheng, Dispersionless manipulation of reflected acoustic wavefront by subwavelength corrugated surface, Sci. Rep. 5 (2015) 10966.
[29] V.S. Malinovsky, D.M. Donskoy, Electro-magnetically controlled acoustic metamaterials with adaptive properties, J. Acoust. Soc. Am. 132 (4) (2012) 2866–2872, https://doi.org/10.1121/1.4744943, http://asa.scitation.org/doi/10.1121/1.4744943.
[30] K.-S. Rossignol, J. Delfs, F. Boden, On the relevance of convection effects for a laser-generated sound source, Am. Inst. Aeronaut. Astronaut. (2015), https://doi.org/10.2514/6.2015-3146.